Available online at www.sciencedirect.com
SCIENCE DIRECT®

Journal of the European Ceramic Society 24 (2004) 2303–2311
www.elsevier.com/locate/jeurceramsoc

Tape casting of AlN–SiC–$MoSi_2$ composites

E. Roncari*, P. Pinasco, M. Nagliati, D. Sciti

CNR–ISTEC, Institute of Science and Technology for Ceramics, Via Granarolo 64, I-48018 Faenza, Italy

Received 4 April 2003; received in revised form 6 August 2003; accepted 14 August 2003

Abstract

Composites in the system AlN–SiC–$MoSi_2$ were produced by tape casting and sintering. The rheological behaviour of the non-aqueous ceramic suspension was investigated, considering different solvent–deflocculant systems. Slurry formulations were optimised changing the ceramic to total volume ratio and the binder to plasticizer ratio. The characteristics of the green tapes, obtained in different conditions, were studied in terms of apparent density, porosity and microstructure. Sintering tests were carried out under nitrogen atmosphere at temperatures of 1800 and 1850 °C. The density and microstructure of the sintered samples is related to the composition of the tape casting slurries, to the processing procedures and to the sintering conditions. The possibility of tailoring the thickness of the sample by lamination of several tapes has also been evaluated.

Keywords: AlN; Composites; Microstructure—final; $MoSi_2$; SiC; Suspensions; Tape casting

1. Introduction

A novel class of electro-conductive ceramics is the group of composites where the conductive phase is molybdenum disilicide. Beside the high electrical conductivity, $MoSi_2$ possesses a high melting point (about 2030 °C) and excellent oxidation resistance at high temperature, which makes it a good candidate for high temperature applications. When $MoSi_2$ is combined with SiC, SiAlON, Al_2O_3, AlN, ZrO_2 or Si_3N_4 [1,2] (as matrix or reinforcement), many relevant properties such as strength, toughness and high temperature behaviour are highly improved. In particular, the combination of $MoSi_2$ with AlN and SiC was found to be promising for applications as heaters and igniters due to suitable electrical characteristics that can be tailored by means of an appropriate SiC/$MoSi_2$ ratio. The essential feature that guarantees the success of these composites is the absence of chemical reaction between the three main compounds and little or no diffusion of cations from one phase to another. In this way, each structure contributes its distinctive characteristic properties to the system and the overall material benefits from the interplay of properties.

The aim of this paper is focused on the possibility to realize thin products by tape casting techniques and sintering in order to evaluate the suitability of new structural electro ceramics to be used for high temperature application.

A literature survey of tape casting slurry with different composition of $MoSi_2$, AlN, SiC, indicates that the ceramic powders were generally dispersed in three kinds of solvent: methyl-ethyl-ketone/ethanol,[3–5] methyl-ethyl-ketone/2-propanol [6,7] and trichloroethylene/ethanol [8] in their azeotropic mixture. A phosphate ester was most frequently used as deflocculant also in the $MoSi_2/Al_2O_3$ suspensions where negatively ($MoSi_2$) and positively (Al_2O_3) charged powder surface were mixed.[3] To ensure the cohesion of the green tapes after the solvent evaporation, polyvinylbutyral polymer[3,6,8] and acrylic resins [7] were used as binder. Different phthalates [3,6] and polyethylene glycol[8] are used as plasticizer for this system to improve the flexibility and workability of the products.

This work highlights the relationships between slurry formulation, rheological behaviour of the suspensions and characteristics of the green tapes. The microstructure of the sintered multilayered sample is discussed in terms of the processing parameters.

* Corresponding author. Tel.: +39-546-699753; fax: +39-546-46381.

0955-2219/$ - see front matter © 2003 Elsevier Ltd. All rights reserved.
doi:10.1016/j.jeurceramsoc.2003.08.004

2. Experimental

2.1. Starting materials

The raw powders used are commercial high-purity products: AlN (grade C, H. C. Starck, Germany), $MoSi_2$ (Aldrich, USA), β-SiC (BF-12, H. C. Starck, Germany) and, as sintering aid, Y_2O_3 (H. C. Starck, Germany). The as received $MoSi_2$ powder was ball milled for 120 h in ethanol and dried to reduce the mean particle diameter from 2.9 to 1.75 μm. The characteristics of the powders are shown in Table 1.

The specific surface area was determined by nitrogen adsorption using BET single point method (Sorpty 1750, Carlo Erba, Italy); the particle size distribution was measured with an X-ray sedimentation technique (Sedigraph 5100, Micromeritics, USA). The phase composition was determined by X-ray diffraction at room temperature (Miniflex Rigaku, Japan). The fracture surface of the samples was analysed by scanning electron microscopy (SEM) (Stereoscan 360, Leica, Cambridge, UK) coupled with an energy dispersive X-ray spectrometer (EDS).

The starting composition of the ceramic composite, selected on the basis of previous works,[1,2] is the following:

[98 wt.% (55 vol.% AlN + 15 vol.% SiC + 30 vol.% $MoSi_2$) + 2 wt.% Y_2O_3]

where Y_2O_3 acts as sintering aid.

The dispersion of ceramic powder in non-aqueous system was studied testing two different solvent systems and two deflocculants. The solvents were: (1) azeotropic mixture of methyl-ethyl-ketone and ethanol (MEK–EtOH, 66:34 vol.%); (2) azeotropic mixture of methyl-ethyl-ketone and 2-propanol (MEK–2PRO, 32:68 wt.%). Phosphate ester (Ep) (Enphos PS610, Crompton, France) and glycerol trioleate (GTO) (Fluka, Switzerland) were tested as deflocculants.

The phosphate ester is derived by reacting phosphoric acid with ethoxylate. The phosphoric acid contains three hydroxyl groups that can be replaced by alkoxy groups to form mono-, di- and triesters that would appear as:

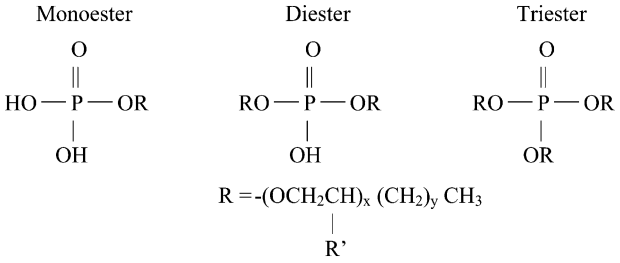

The alkoxy chain is ramified with an unspecified R′. The alkoxy chain contains both a polyoxyetilene group (x) with hydrophilic behaviour and an alkyl group (y) with lipophilic behaviour. The EP used in this work is a combination of monoesters and diesters with a density of 1.11 g/cm.[3] The GTO is the esterification product of the glycerol with oleic acid.

The poly-vinyl-butyral (PVB) (B98, Monsanto, USA) was selected as a binder as it gives excellent green tape characteristics. According to the experimental composition for tape casting technology [9–12] polyethylene glycol (PEG-400, Merk, Germany) and benzyl butyl phthalate (BBP) (S160, Monsanto, USA) were used as plasticizer in 1:1 weight ratio.

2.2. Rheological measurements

The rheological properties of the ceramic suspensions were measured using a controlled rate rheometer with coaxial cylinders. All samples were initially shear stressed at the maximum value (500 s^{-1}) for 1 min. Flow curves were recorded at 25 °C by testing the samples at shear rates ranging from 0.0 to 500.0 s^{-1}, for 10 min sweep, up and down sequence. The suspensions of 35 vol.% solids loading and fixed 1.0 wt.% concentration of deflocculant (referred to the dry powder), in the two different dispersants, were tested immediately after 15 h of ball milling. Only for the system MEK-EtOH and GTO the solid loading was decreased to 32 vol.%.

The optimal deflocculant concentration was found by conductivity measurements performed at 25 °C using an electronic conductance meter with platinum coated electrodes and the cell constant was determined with 0.1 M KCl standard solution. The ceramic suspensions (10 vol.%) at different deflocculant concentrations were obtained after ball milling for 20 h. The conductivity of the slurry and supernatant obtained after centrifugation was measured. The starting ceramic powders were separately tested at 0.0 wt.% of deflocculant concentration.

2.3. Slurry preparation and tape casting procedure

In order to avoid competitive adsorption, ceramic powder was first added to the solvent–deflocculant

Table 1
Physical chemical characteristics of ceramic powders

Powder	Specific surface area (m^2/g)	Mean diameter (μm)	Density (g/cm^3)	Crystalline phase
$MoSi_2$[a]	2.8	1.76[b]	6.27	Tetragonal
β-SiC	11.6	0.80	3.21	cubic
AlN	4.1	2.30	3.26	Hexagonal
Y_2O_3	13.2	0.45	5.03	cubic

[a] Ball milled for 120 h.
[b] As received: 2.9 μm.

solution and ball milled with silicon nitride milling media. The addition of PVB binder and plasticizer to the ceramic suspension was done 14 and 34 h respectively after the mixing started and the whole mixture was then left to homogenise for an additional 8 h. The slurry was subjected to a vacuum to remove trapped air bubbles, than filtered directly into the reservoir of the casting unit and cast, with a blade high of 0.6 mm, onto a silicone coated Mylar® moving at a casting speed of 65 cm/min. The tapes were allowed to dry for 12 h at room temperature without airflow to prevent crack formation as a consequence of rapid solvent evaporation from the upper surface.

Tape casting slurries were prepared by varying the inorganic to organic ratio (X) (equal to the volume of the ceramic powder divided by the total volume of ceramic, deflocculant, binder and plasticizer), and the binder to plasticizer volume ratio (Y). The benzyl butyl phthalate and polyethylene glycol were introduced in the slurry as plasticizer, in the 1:1 weight ratio. The slurries compositions are reported in Table 2. The viscosity of the slurries was kept similar by adjusting the amount of solvent.

Circular pieces with a diameter of 40 mm were punched out from the as-cast green tapes. These pieces were then stacked and laminated by pressing at 75 °C and 30 MPa for 30 min to obtain 10-layer laminated structure.

The green density (ρ_g) was geometrically determined. The apparent green density (ρ_g app) was expressed by the W_p/V ratio where W_p is the ceramic powder weight obtained from the slurries formulations and V is the real volume of the sample.

The amount of porosity in the green tapes was determined assuming that the total volume of the samples is the sum of the ceramic, organic components and porosity volume.

2.4. Debonding, sintering and microstructural analyses

Thermo gravimetric analysis (STA409, Netzsch, Germany) of all the organic additives and a sample of the green tape richer in organic components were performed in a nitrogen atmosphere.

Table 2
Slurry composition at different X and Y values

Component	Composition (vol.%)						
	1	2	3	4	5	6	7
Ceramic powder	25.35	27.49	26.84	27.74	28.64	28.17	27.63
Deflocculant	0.95	1.03	1.01	1.04	1.07	1.06	1.04
PVB	5.64	4.78	5.25	4.87	4.49	4.82	5.20
PEG + BBP	7.05	5.97	5.25	4.87	4.49	4.02	3.47
Solvent	61.00	60.73	61.65	61.48	61.30	61.93	62.66
X	0.65	0.70	0.70	0.72	0.74	0.74	0.74
Y	0.80	0.80	1.00	1.00	1.00	1.20	1.50

Thermal treatments, including the burnout stage (600 °C, 1 h) and the sintering stage at various temperatures (1800–1850 °C) with 0.5–1 h of holding time, were carried out in graphite furnace under nitrogen atmosphere. In order to prevent dissociation of AlN, a powder bed (AlN + BN) was used. The density of the sintered materials (ρ_s) was measured by Archimedes method in water. residual porosity was estimated through image analysis (Image Pro-plus 4.0, Media Cybernetics, USA).

The microstructure of the manufactured specimens was analysed by X-ray diffraction and scanning electron microscopy on polished surfaces and cross sections.

3. Results

3.1. Dispersant and deflocculant selection

Considering that SiC and $MoSi_2$ show a silica like surface, it is expected that both powders exhibit a similar dispersion behaviour related to their negatively charged surface. On the other hand AlN and Y_2O_3 powder surface are positively charged and consequently the differences in the characteristics of $MoSi_2$-SiC and AlN-Y_2O_3 powder surfaces should results into a different interaction with organic additives. Between the two deflocculants tested, the Ep plays both roles; (1) as an anionic deflocculant, attracting the positively charged surface by coulomb forces followed by a dissociation mechanism in which hydronium H_3O^+ ions are liberated into the solvent, and (2) as a steric dispersant, by anchoring the chain molecules to the particle surfaces.[13] The GTO, a non-ionic deflocculant, was tested for its pure steric stabilization mechanism.

Two different solvent systems were considered by coupling the high dielectric constant ($\varepsilon = 15.5$) and the good binder dissolution ability of MEK with high hydrogen bonding strength of alcohols like EtOH and 2PRO. The differences between the two alcohols are a higher dielectric constant (24.30 versus 18.8) and a lower viscosity (1.07 mPas versus 2.04 mPas) for EtOH with respect to 2PRO, while the boiling point, density and surface tension remain quite similar.

The slips were dispersed with 1 wt.% of deflocculant and a solid loading of 34 vol.%.

Although the dispersing conditions of each system were not yet optimised, it is expected that for any other deflocculant concentrations the viscosity values can change, but always maintaining the same relative order and tendency. The strong influence of the solvent and deflocculant properties on the suspension rheology is shown in Fig. 1.

All the suspensions show a pseudoplastic behaviour with almost no time dependence effect. The maximum

viscosity corresponds to MEK–EtOH and GTO system whose solid loading concentration was decreased to 32 vol% to prevent the formation of a too viscous suspension. MEK–2PRO solvent system shows, at 100 s^{-1}, a medium viscosity value, in particular using GTO as deflocculant the slurry have a lower viscosity (183 mPas) in comparison to the suspension with Ep (251 mPas).

The slip prepared with Ep deflocculant in MEK–EtOH has very low viscosity in all the shear rate range tested. According to these results, the MEK–EtOH as dispersant and phosphate ester as deflocculant for the ceramic slips were chosen.

3.2. Optimum deflocculant concentration

The conductivity test performed on the composite slurry (10 vol.%), at 0.0 wt.% of deflocculant, is quite different from that of the solvent alone as shown in Fig. 2. The increase in conductivity must be due only to ions brought in by the ceramic powders. Furthermore the additions of small amount of deflocculant to the solvent do not change the conductivity confirming that the ions are not introduced by the deflocculant but by the ceramic system.

Suspensions of SiC, AlN and Y_2O_3 powders (10 vol.%) show conductivity quite similar to the solvent (Table 3) excluding these powders as possible ions releasers.

Because the $MoSi_2$ powder was used in the composite formulation after a ball milling process for 120 h, both $MoSi_2$ as received and ball-milled powders ($MoSi_2$-b) were conductively tested at the same concentration realized in the composite (2.95 vol.%). The high conductivity value showed by the milled $MoSi_2$-b (46.6 μS cm^{-1}) can be attributed to a modified and ionisable $MoSi_2$ surface. Show et al. showed that the oxidation of $MoSi_2$ could arise at room temperature leading to a final formation of a duplex oxide layer of $SiO_2 + MoO_3$ covering the ceramic surface.[14]

In particular the MoO_3 oxide reacts with water, present in the solvent or adsorbed from the atmosphere, to release H^+ and MoO_4^{2-} ions as the following reaction

$$MoO_3 + H_2O \rightarrow MoO_4^{2-} + 2H^+$$

This behaviour, can explain the high conductivity of the treated $MoSi_2$.

On the other hand the positive charge of AlN powder was explained [5] by the interaction between amphoteric OH groups present on the AlN surface and H^+ ions following the acid base reaction

$$AlOOH + H^+ \rightarrow AlOOH_2^+$$

The ability of the AlN surface to capture the H^+ ions explains the decreased conductivity value of the AlN/$MoSi_2$-b suspension at the same volume concentration used in the composite slurry formulation (Table 3). The conductivity of the composite slurry arises from the surface modification of the $MoSi_2$ powder during the milling process followed by a quite complete neutralization by means of AlN powder.

A small addition (0.2 wt.%) of deflocculant to the AlN/$MoSi_2$-b suspension decreases the conductivity and the same behaviour is found for the composite slurry that shows a minimum value at about 0.5 wt.% of deflocculant concentration (Fig. 2). Further work is in progress to elucidate the Ep interactions involved with

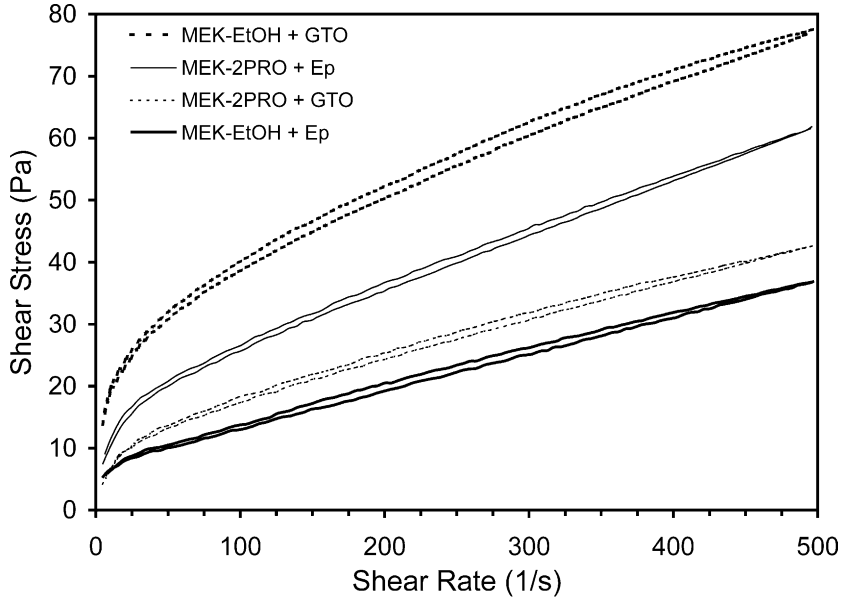

Fig. 1. Rheological curves for ceramic slurries with different solvent system and deflocculant.

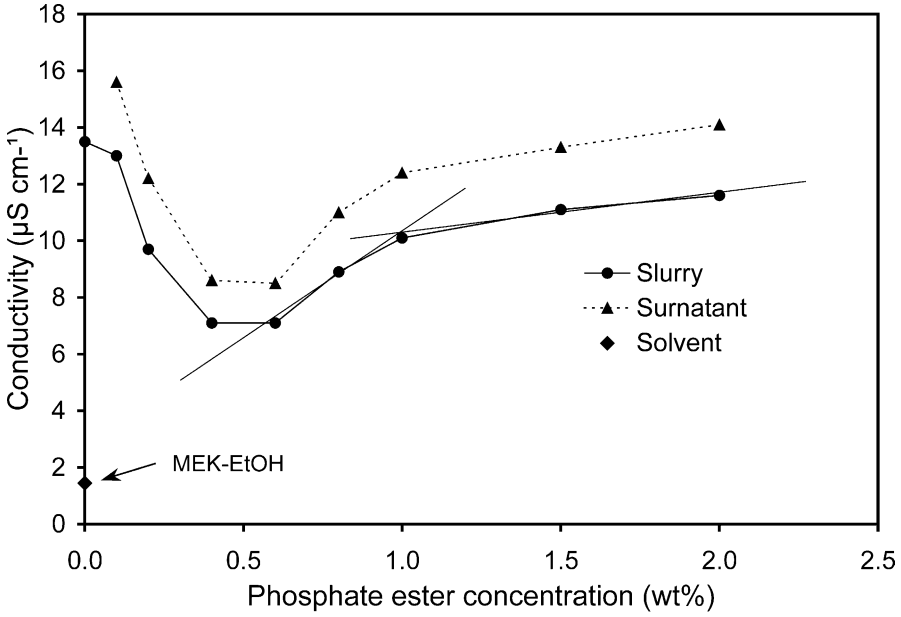

Fig. 2. Electrical conductivity of slurry composite and surnatant versus phosphate ester concentration.

Table 3
Conductivity of the ceramic suspensions at 0.0 vol% deflocculant concentration

Powder	Type	Concentration (vol%)	Conductivity (μS cm^{-1})
AlN	a	10	3.53
SiC	a	10	1.15
Y_2O_3	a	10	0.50
$MoSi_2$	a	2.95	16.80
$MoSi_2$	b	2.95	46.60
$MoSi_2$/AlN	b/a	2.95/5.41	10.50
Composite	b	10	13.50
Solvent system	=	100	1.45

a, As received; b, Ball milled for 120 h and dried.

all the ceramic surfaces present in the suspension. For Ep concentration higher than 0.5 wt.% the electrical conductivity increases according to the model showing that the deflocculant is not extensively ionised until it is adsorbed onto the polar surface of the powder.[9]

The Ep attaches to the particle through the phosphate group and the powder surface apparently acts as a catalyst for dissociation of the deflocculant with a consequent increase in the ion concentration. When the ceramic surface coverage is achieved, the Ep does not easily reach the surface; the ionisation increases only slowly with increasing Ep concentration.

The conductivity of the supernatant and the slurry are quite similar with lower value for slurry due to insulating properties of composite powders.

In order that a monolayer of deflocculant with the head of the molecule is strongly adsorbed on the powder surface, a phosphate ester concentration of about 1.0 wt.% is enough and this value was considered for all tape casting formulations.

3.3. Casting behaviour and tape characterization

Slurry composition at different X and Y values is reported in Table 2.

With the aim to obtain final dense sintered samples firstly X value was increased from 0.65 to 0.70 with the same 0.8 Y value (1–2). Since a good joining of the layers during lamination was obtained using tape with a low quantity of plasticizer[15] a second series of formulations (3–5) was studied increasing X value from 0.70 to 0.74 but using a higher quantity of binder (Y value fixed to 1.0). Finally three formulations, decreasing the plasticizer content (5–7) at the same X value of 0.74, were obtained to improve the lamination ability of the tapes.

Independently of the X and Y values, all the suspensions were easily cast and the dry tapes were peeled away from the Mylar support without any adhesion phenomena. All tapes are crack-free with a flexibility decreasing for high X values.

High green density, low porosity and good lamination ability are characteristics difficult to obtain together.

Increasing the ceramic volume concentration (X) with constant Y value, the green and apparent density of the tapes increases as a consequence of the higher ceramic volume in the same total volume (formulation 1 and 2 in Table 4). An opposite trend is observed in the 3–5 formulations where a different concentration of organic additives and especially a reduced amount of plasticizer in relation to the binder prevent the optimum packing of the ceramic particles.

The second set of formulations (2–3 and 5–7) shows that the apparent green density decreases and porosity increases with increasing Y value, as reported in Table 4. In fact a low amount of plasticizer prevents an easy flow of the ceramic particles with the consequent difficult particle rearrangement. When Y increases the particle rearrangement is too small to allow an optimum in packing density.

As mentioned above the plasticizer plays an important role in the tape process, the reduction of its amount in relation to the binder increases the viscosity of the slurry. This influences also the relative green density of the cast slurry: a slurry of low viscosity results in higher relative green density, if the amount of all other components is constant. Furthermore the plasticizer acts as a lubricant between the individual layers, which limits the bonding during lamination.[15] Therefore low Y value compositions lead to delaminated substrates.

Lamination process increases the green density (30 MPa for 30 min at 75 °C), softening the organic component and pressing the powder particles, promoting a better particles packing as results from the green density values of the 10-layered samples.

A higher green density near to the top surface of dried tapes was not observed; the ceramic powders are homogenously distributed in the tape thickness. The multilayer section shows no concentration gradient of $MoSi_2$ suggesting that $MoSi_2$, whose density and particle size are higher than the other compound, does not settle during the drying stage.

3.4. Burn out and sintering behaviour

The thermo gravimetric analysis (TGA), reported in Fig. 3, shows that the organic components have a different range of decomposition temperature. The deflocculant burns out at lower temperature in the 200–280 °C range followed by the first plasticizer, where decomposition arises between 240 and 380 °C. The binder starts to decompose when the elimination of first plasticizer is complete. Consequently the burnout process takes place in the best way because the coming out of the organic additives at lower temperature allows an easier elimination of the binder that use the channels so formed.

Furthermore it is important for the individual organic additives to be burnout at different temperatures but within a narrow temperature range, in order to avoid disturbing the powder structure in the tape. The decomposition process of a green tape (formulation 1) is shifted to lower temperature (160 °C) essentially due to the catalytic effect of inorganic surfaces linked with the capillary-driven transport presents in the ceramic green body.[16] The burnout continues in only one step until 400 °C, then a second step arises in the 400–600 °C temperature range due to the residual deflocculant and second plasticizer final decomposition. After 600 °C the weight of the sample increases rapidly for the extreme reactivity of the composite with a very small oxygen quantity present in the nitrogen atmosphere of the thermo gravimetric apparatus. The total weight loss is 9%, lower than theoretical 12.5%, due to the incomplete elimination of decomposition products in nitrogen atmosphere below 700 °C. According with TGA results, different thermal treatments (Table 5) were tested. The best results, in terms of final density, were obtained with a heating rate of 150 °C/h until 600 °C followed by a hold for 30 min. Slower heating rate, as 120 °C/h and in particular 60 °C/h, used for the 0.65/0.8 and 0.70/0.8 formulation respectively, do not contribute to increasing the final density of the products. After the elimination of the organic components, densification occurs via liquid phase sintering. The sintering additive, Y_2O_3, reacts with Al_2O_3 and the SiO_2 present in AlN, $MoSi_2$ and SiC starting powders, forming either a Y_2O_3–rich aluminosilicate liquid (in the ternary phase diagram SiO_2–Al_2O_3–Y_2O_3 a eutectic is present at 1400 °C), or an oxynitride melt.

The densities of the sintered multilayers samples ranged from 78 to 94% of theoretical (see Table 5), depending on solid loading and sintering conditions. The best relative density was 94.5% for a multilayer (10 layers) obtained after sintering at 1850 °C for 30 min, with solid loading $X = 0.65$. When X is higher than 0.65 the density decreases and a higher residual porosity is found in the final products.

Lower densities (65–80%) were obtained when the samples were sintered at 1800 °C. Moreover a slow binder burnout was also found to be detrimental for densification.

Table 4
Density and porosity of the monolayer green tapes

Formulation X/Y	Code	ρ_g (g/cm^3)	ρ_g app (g/cm^3)	ρ_g app (%)	Porosity (%)
0.65/0.8	1	2.053	1.794	43.03	33.79
0.70/0.8	2	2.284	2.049	49.14	29.74
0.70/1.0	3	2.249	2.019	48.42	30.79
0.72/1.0	4	2.015	1.826	43.78	39.12
0.74/1.0	5	2.012	1.839	44.11	40.49
0.70/0.8	2	2.284	2.049	49.15	29.74
0.70/1.0	3	2.249	2.019	48.42	30.79
0.74/1.0	5	2.012	1.839	44.11	40.49
0.74/1.2	6	1.982	1.813	43.46	41.19
0.74/1.5	7	1.911	1.748	41.91	43.29

3.5. Microstructural characterization

The main crystalline phases detected are: β-SiC, tetragonal $MoSi_2$, hexagonal AlN and YAG. Traces of crystalline $Mo_{\leqslant 5}Si_3C_{\leqslant 1}$ and different of SiAlON politypes were also found. Independently on the presence of

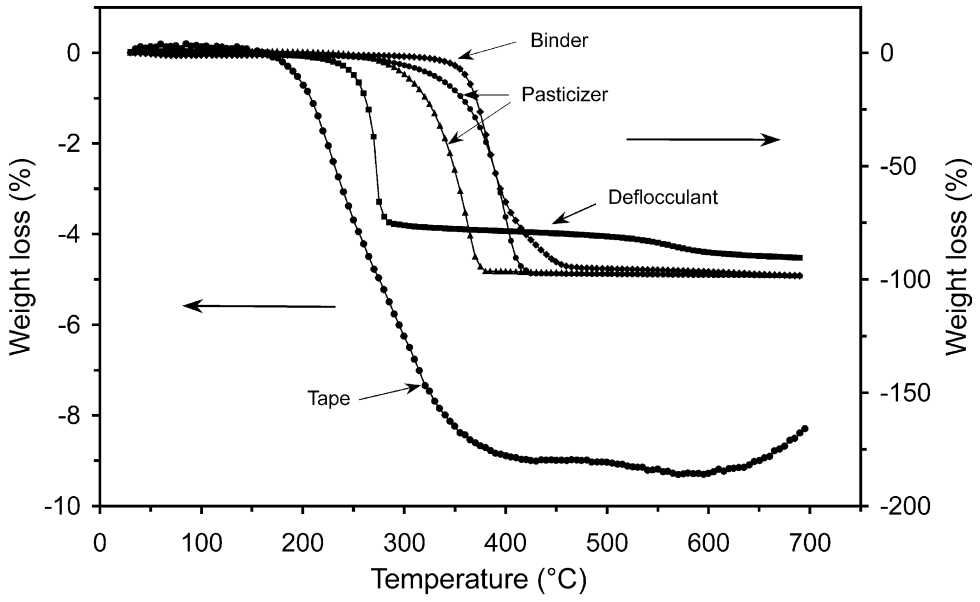

Fig. 3. TG curves of a green tape (0.65/0.8 formulation) and the organic additives.

Table 5
Sintering conditions and density values of multilayers

Formulation	Burn out			Sintering		ρ_s	
X/Y	°C/h	T (°C)	t (min)	T (°C)	t (min)	(g/cm^3)	(%)
0.65/0.8	120	500	30	1800	30	3.63	87.05
0.65/0.8	60	600	120	1800	30	2.71	64.99
0.65/0.8	150	600	30	1850	30	3.94	94.48
0.70/0.8	120	500	30	1800	30	3.24	77.72[a]
0.70/0.8	60	600	120	1800	30	3.34	80.10
0.70/1.0	150	600	30	1850	30	3.91	93.77
0.70/1.0	150	600	30	1850	60	3.77	90.41
0.72/1.0	150	600	30	1850	30	3.77	90.43
0.74/1.0	150	600	30	1850	30	3.83	91.73
0.74/1.2	150	600	30	1850	30	3.61	86.45
0.74/1.5	150	600	30	1850	30	3.64	87.36

[a] Delamination.

residual porosity, SEM analysis of the fractured tapes, revealed that, in all the samples, the $MoSi_2$ distribution is homogeneous all over the section, i.e. no difference was observed between the upper and the lower surface. The multilayered samples exhibited a perfect adhesion between the different layers. Moreover, neither traces of the junction between overlapping layers nor interfacial delaminations were observed after sintering in the multilayered samples, such that these materials resemble bulk materials.

Fig. 4 compares the fracture surfaces of samples sintered at 1800 °C/30 min (Fig. 4a) and 1850 °C/30 min (Fig. 4b). Samples treated at 1800 °C show high residual porosity. In contrast, composites treated at 1850 °C have a more homogeneous microstructure with rounded grains and limited porosity. No significant differences were observed for composites treated at 1850 °C/1 h in comparison with those sintered at the same temperature for 30 min.

An example of polished cross sections is shown in Fig. 5 a–b, where the bright contrast phase is molybdenum disilicide and the grey regions consist of the AlN and SiC phases. The dark regions are residual pores.

Fig. 5b highlights the presence of further phases randomly distributed among the three main phases (AlN, SiC, $MoSi_2$), in the areas distinguished by an intermediate contrast. EDS analyses carried out in different regions revealed the presence of Si, Al, N, O and Y, but the relative amounts of these elements is not constant throughout the material. These compounds originated from the liquid phase formed during sintering and are most probably SiAlON, Y-SiAlON or YAG phases.

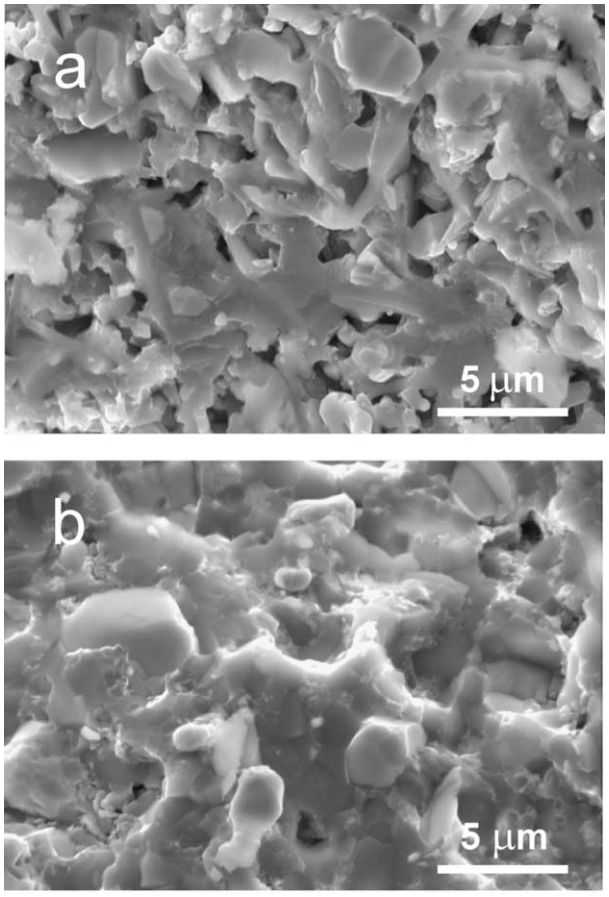

Fig. 4. SEM micrograph of a fracture surface; (a) 0.70/0.8 sample sintered at 1800 °C for 30 min; (b) 0.70/1.0 sample sintered at 1850 °C for 30 min.

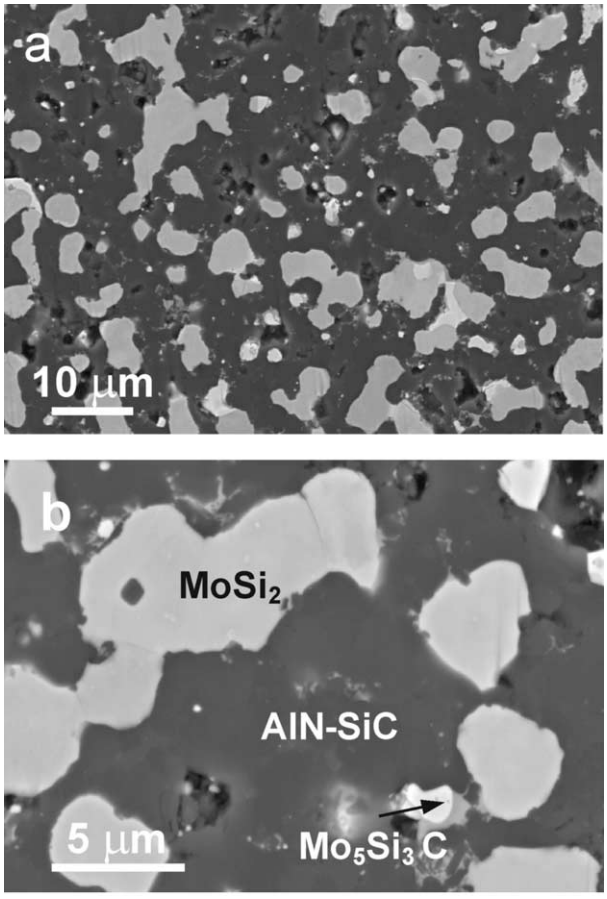

Fig. 5. Backscattered electron images of polished surface of a 94% dense multilayer sample (0.70/1.0). The bright contrast phase is $MoSi_2$.

No micro cracks were observed either at the boundaries between SiC and AlN that possess very close lattice parameters and thermal expansion coefficient ($4.5{\cdot}10^{-6}\ ^{\circ}K^{-1}$ and $5{\cdot}10^{-6}\ ^{\circ}K^{-1}$ respectively) or between the matrix and $MoSi_2$ despite its relatively high thermal expansion coefficient ($9{\cdot}10^{-6}\ ^{\circ}K^{-1}$).

EDS analysis revealed variations in Mo content in $MoSi_2$ particles (Fig. 5a). The brighter region of the $MoSi_2$ particles contains a higher concentration of Mo. According to previous results on similar materials[2] the lighter contrast phase found in region is presumably $Mo_{\leqslant 5}Si_3C_{\leqslant 1}$. This feature is probably due to several factors: (1) residual carbon is left by the organic species after debonding, (2) the samples are in contact with graphite elements used as support, (3) the furnace environment is C-rich.

The shape of the $MoSi_2$ inclusions is irregular, their mean dimensions (estimated by image analysis) range from 1.3 to 1.7 μm. Comparing these values with the size distribution of the starting $MoSi_2$ powder (after the milling procedure), it became apparent that the $MoSi_2$ particles underwent small coarsening during sintering.

4. Conclusions

Composites AlN–SiC–$MoSi_2$, with 55/15/30 volume concentration respectively, have been fabricated via the tape casting method. Both the slurry formulations and the sintering conditions were optimised to improve the final product densities. Regarding the slips the best dispersion was achieved using an azeotropic mixture of MEK–EtOH as a dispersant and a phosphate ester concentration of 1.0 wt.% (referred to the solid) as deflocculant. The optimum ceramic volume concentration was 70% with a relative binder to plasticizer ratio of 1.0, where neither adhesion of the tape nor cracking are observed. Mono and multilayers structures, after lamination at 75 °C and 30 MPa for 30 min, were obtained. The best burnout conditions were found with a heating rate of 150 °C/h until 600 °C (dwell for 30 min). The sintered multilayers densities range from 78 to 94% depending on the solid loading and the thermal treatment. The microstructure of the sintered samples was then related to the slurry composition, process parameters and sintering conditions.

References

1. Sciti, D., Guicciardi, S. and Bellosi, A., Microstructure and properties of Si_3N_4- $MoSi_2$ composites. *J. Ceramic Processing Research*, 2002, **3**, 87–95.
2. Sciti, D., Guicciardi, S., Melandri, C. and Bellosi, A., Development of high-temperature resistant composites in the system AlN–SiC–$MoSi_2$. *J. Am. Ceram. Soc.* (submitted for publication).
3. Dumont, A. L., Bonnet, J. P., Chartier, T. and Ferreira, J. M. F., $MoSi_2/Al_2O_3$ FGM: elaboration by tape casting and SHS. *J. Eur. Ceram. Soc.*, 2001, **212**, 2353–2360.
4. Reynaud, C., Thevenot, F., Chartier, T. and Besson, J.L. Preparation and microstructure of liquid phase sintered SiC laminar materials. In *Key Engineering Materials* Vols 206–213, Trans Tech Publications, Switzerland, 2002, pp. 1017–1020.
5. Descamps, M., Monreau, G., Mascart, M. and Thierry, B., Processing of aluminium nitride powder by the tape-casting process. *J. Eur. Ceram. Soc.*, 1994, **13**, 221–228.
6. Zhang, G. J., Yue, X. M. and Watanabe, T., Al_2O_3/TiC/($MoSi_2 + Mo_2B_5$) multilayer composites prepared by tape casting. *J. Eur. Ceram. Soc.*, 1999, **19**, 2111–2116.
7. Shaw, L. and Abbaschian, R., Fabbrication of SiC-whisker-reinforced $MoSi_2$ composites by tape casting. *J. Am. Ceram. Soc.*, 1995, **78**(11), 3129–3132.
8. Stuffe, S. and Wilkinson, D. S., $MoSi_2$-based sandwich composite made by tape casting. *J. Am. Ceram. Soc.*, 1995, **78**(11), 2967–2972.
9. Cannon, W.R., Becker, R. and Mikeska, K.R. Interaction among organic additives used for tape casting. In *Advances in Ceramics*, Vol 26, Ceramic Substrates and Packages for Electronic applications. American Ceramic Society, Westerville, Ohio, 1989, pp. 525–541.
10. Mistler, R. E., Shanefield, D. J. and Runk, R. B., Tape casting of ceramics. In *Ceramic Processing Before Firing*, ed. G. H. Onoda and L. L. Hench. , 1978, pp. 411–448.
11. Moreno, R., The role of slip additives in tape casting technology: I. solvents and dispersants. *Am. Ceram. Soc. Bull.*, 1992, **71**(10), 1521–1534.
12. Moreno, R., The role of slip additives in tape casting technology: II. binders and plasticizers. *Am. Ceram. Soc. Bull.*, 1992, **71**(11), 1647–1657.
13. Mikeska, K. and Cannon, W. R., Dispersants for tape casting pure barium titanate. In *Advances in Ceramics, Vol. 9,* Forming of ceramics, ed. J. A. Mangles. American Ceramic Society, Columbus, OH, 1984, pp. 164–183.
14. Shaw, L. and Abbaschian, R., Chemical states of the molybdenum disilicide ($MoSi_2$) surface. *J. Mater. Sci.*, 1995, **30**, 5272–5280.
15. Chartier, T., Streicher, E. and Boch, P., Preparation and characterization of tap cast aluminium nitride substrates. *J. Eur. Ceram. Soc.*, 1992, **9**, 231–242.
16. Lewis, J. A., Binder removal from ceramics. *Annu. Rev. Mater. Sci.*, 1997, **27**, 147–173.